NASA

Technical Memorandum **79699**

Motions of Charged Particles in the Magnetosphere Under the Influence of a Time-Varying Large Scale Convection Electric Field

Paul H. Smith, N. K. Bewtra, and R. A. Hoffman

JANUARY 1979

National Aeronautics and Space Administration

Goddard Space Flight Center
Greenbelt, Maryland 20771

ABSTRACT

The motions of charged particles under the influence of the geomagnetic and electric fields are quite complex in the region of the inner magnetosphere. The Volland-Stern type large scale convection electric field ($\vec{E} = -\nabla\Phi$ and $\Phi = AR^{\gamma} \sin\phi$) with $\gamma = 2$ has been used successfully to predict both the plasmapause location and particle enhancements determined from Explorer 45 (S^3-A) measurements. We have recently introduced into the trajectory calculations of Ejiri et al. (1978) a time dependence in this electric field based on the variation in Kp for actual magnetic storm conditions. The particle trajectories are computed as they change in this time-varying electric field. Several storm "fronts" of particles of different magnetic moments are allowed to be injected into the inner magnetosphere from L = 10 in the equatorial plane. The motions of these fronts are presented in a movie format. The local time of injection, the particle magnetic moments and the subsequent temporal history of the magnetospheric electric field play important roles in determining whether the injected particles are trapped within the ring current region or whether they are convected to regions outside the inner magnetosphere.

INTRODUCTION

Particle convection in the magnetosphere has been discussed by a number of authors since the early convection models of Dungey (1961), and Axford and Hines (1961), and its significance in the dynamics of the magnetosphere is well recognized. The review on this subject by Axford (1969) provides quite extensive discussion and references to the many important papers up to that time. Chappell (1974) reviewed the direct and indirect measurements of the convection electric field that were made since Axford's (1969) review, and discussed the way in which the measurements supported the basic convection theory. Two works of special importance in the early quantitative modeling of magnetospheric processes are those by Kavanagh et al. (1968) and Chen (1970). Kavanagh et al. (1968) developed a simple analytical model which combined a large scale uniform electric field, similar to that given by Brice (1967) with a corotation electric field and the geomagnetic field given by Mead (1964). Chen (1970) presented in detail the motions of low energy protons in a dipole geomagnetic field under the superimposed convection and corotation electric fields and showed that the trajectories of these low-energy protons are topologically quite different from those of other classes of particles. As an extension of these works, principally that of Kavanagh et al. (1968), Wolf (1970) added another dimension by considering the ionospheric conductivity effects on the convective flow patterns of magnetospheric plasma. The theory of convection in the magnetosphere had become so well established based on the various works indicated above and in the reviews by Kivelson (1976) and Stern (1977) that it became generally accepted that the source of the ring current protons

associated with the main phase magnetic storms was the convection of plasma sheet protons into low L values (Axford, 1969; Vasyliunas, 1972; Nishida and Obayashi, 1972), even though there had been almost no direct experimental measurements of the characteristics of these storm time ring current particles that would substantiate this concept. The characteristic features of the initial enhancement of the storm time ring current particles in the evening hours became available through the Explorer 45 (S^3-A) program and the measurements were found to be qualitatively consistent with the flow patterns resulting from a combination of inward convection, gradient drift, and corotation (Smith and Hoffman, 1974).

In more recent years, one aspect of this convection theory has come into question, that is, the source of the particles. The discoveries of ions in the magnetosphere heavier than hydrogen (Shelley et al., 1972) and ion and electron beams directed up along magnetic field lines from the atmosphere (Johnson et al., 1977; McIlwain, 1975) have suggested that the ionosphere may be a source for ring current particles, rather than, or in addition to, the plasma sheet.

This paper briefly traces the evolution of the work of a number of researchers which has lead from the stage of qualitative agreement to a stage of quantitative agreement between the convection theory and measurements of related magnetospheric phenomena. Facets of the evolution have been described in the review by Kivelson (1976) on the variation of magnetospheric electric fields with geomagnetic activity and in the extensive review by Stern (1977) on the theoretical concepts of

large-scale electric fields. Ejiri (1978) and Ejiri et al. (1978) have developed a quantitative convection model based on Explorer 45 observations. A static electric field is used in this model and the particles move in time (and space) along fixed trajectories. In the situations where the electric field, parameterized by Kp, is fairly constant over a time period of several hours, this is a reasonable approach (Maeda et al., 1978). A time-dependent electric field is needed, however, for the description of the particle trajectories associated with magnetic storms which have a several day duration and decreasing convection electric field (Smith et al., 1978), and for transiently intensified electric fields of substorm time scales (Roederer and Hones, 1974).

In the present paper the approach we have employed to add a large-scale time-dependent convection electric field is described. We have also developed along with this approach a technique for the visual description of the complex motions of the charge particles. By using a computer-generated motion picture of storm "fronts" of injected particles of various magnetic moments we have produced both an educational tool to demonstrate the convective motion of particles in the ring current region and an analytical tool for future studies of particle dynamics.

FORMULISM AND BASIC ASSUMPTIONS

The basic formulism which we use for the computation of the trajectories of charge particles in the magnetosphere is given by Ejiri (1978) and this same computation has been used by Maeda et al. (1978) for electron trajectories. In the equation of motion for the particles it is assumed that non-electromagnetic forces such as gravitational forces, etc. are negligible and that the particles can be represented non-relativistically. It is assumed that the particle motion is adiabatic, i.e. the first and second invariants (magnetic moment and longitudinal invariant) are conserved, and that changes in the electric and magnetic fields are slow and the particle motion can be represented as a motion of its guiding center. The following constraints and conditions are also imposed:

1. The geomagnetic field, B, is an earth centered dipole magnetic field with the same axis as the earth's rotation axis and the magnetic field lines are equipotentials.
2. There are no local energization or loss processes (e.g. charge exchange, wave-particle interactions or collisional loss processes).

The drift velocity, $\vec{u}$, in the equatorial plane is obtained by averaging over a cyclotron motion and a bouncing motion and is given by

$$\vec{u} = \frac{\vec{F} \times \vec{B}}{qB^2} \qquad (1)$$

The force, $\vec{F}$, on the particles is given by

$$\vec{F} = q\vec{E} - q(\vec{\omega}x\vec{R})\,x\vec{B} - W \cdot G(\alpha_o) \cdot \frac{\nabla B}{B} \qquad (2)$$

where,

$\vec{R}$ is the radial vector from the center of the earth,

$\vec{\omega}$ is the angular velocity of the earth's rotation,

$G(\alpha_o)$ is the term associated with the helical path off the equator over the bouncing motion of the particle. It is a function of the particles' equatorial pitch angle, α_o,

W is the kinetic energy of the particle and can be written as $W = \frac{\mu B}{\sin^2 \alpha_o}$, μ is the magnetic moment of the particle. The reader is refered to Roederer (1970) for more detailed discussion on the dynamics of geomagnetically trapped particles.

The first term in Eq (2) is the large-scale convection electric field force which will be discussed below, the second term is the corotational electric force and the third term represents the magnetic curvature and gradient drift forces. When the equatorial pitch angle of the particles is 90°, the last term in equation (2) becomes $-\mu\nabla B$. Note that only equatorially mirroring particles are considered in this paper. This restriction does not apply to the general formalism of Ejiri (1978).

CONVECTION ELECTRIC FIELD MODEL

A simple model of the convection electric field of the magnetosphere has been proposed (Volland, 1973; Stern, 1974, 1975). This Volland-Stern model assumes that the large-scale convection electric field, $\vec{E}_{conv}$, is derivable from a quasi-static electric potential, Φ :

$$\vec{E}_{conv} = -\nabla\Phi_{conv} \qquad (3)$$

and that there is an absence of electric fields parallel to the geomagnetic field lines, $\vec{E} \cdot \vec{B}_o = 0$, where B_o is assumed for convenience to be a coaxial dipole geomagnetic field. This model is also valid only for closed magnetic field lines and within ten earth radii. The scalar potential in the equatorial plane can then be written as

$$\Phi_{conv} = AR^{\gamma} \sin \phi \qquad (4)$$

where R is the equatorial radial distance in earth radii and A is a coefficient which determines the electric field intensity. This coefficient will be discussed in more detail below. The local time dependence is given by the azimuthal angle, ϕ, with $\phi = 0$ at midnight. The value of the exponent, γ, distinguishes this Volland-Stern model from the uniform dawn to dusk electric field. The uniform field used by Chen (1970) is obtained if $\gamma = 1$. Stern (1974) suggested $\gamma = 2$ from a consideration of the OGO-6 measurements of the electric field at high latitudes (Heppner, 1972). Volland (1973) arrived at the same value for γ from a best fit to the shape of the plasmapause and Ejiri et al. (1978) in an analysis of the shape and location of the pre-midnight plasmapause measured by Explorer 45, determined an average value of

γ to be 2.4. The configuration of this large-scale convection electric field, $\vec{E}_{conv}$, is shown in Figure 1 for a normalized value for A and with $\gamma = 2$. The effect of the radial dependence and local time effect are easily seen in this diagram.

In order to account for changes in the convection electric field associated with changes in magnetic activity, Grebowsky and Chen (1975) concluded that the model parameter, A, must be related to some geophysical parameter which describes changes in the large-scale convection. Based on previous correlations with Kp (Carpenter and Park, 1973, Kivelson, 1976), they chose to relate A to the Kp index. By fitting the midnight plasmapause locations measured by the spectrometers on OGO-3 and OGO-5, Grebowsky and Chen (1975) determined the following quadratic dependence on Kp:

$$A = 0.045/ (1 - 0.159Kp + 0.009Kp^2)^3 \qquad (5)$$

where the units of A are kV/R_E^2. In Figure 2 we show the plot of A vs. Kp as well as the resultant $|\vec{E}|$ and L_o, the stagnation distance at dusk, from Figure 4 of Maeda et al. (1978).

The Kp index, which is constructed to indicate global magnetic activity, using the 3 hour values from 12 middle latitude geomagnetic observations to eliminate longitudinal variations, is actually a good indicator of the magnetosphere electric field intensity. It is interesting to note that the intensification of the magnetospheric electric field is the source of the enhancement of geomagnetic activity, in contrast to Dst, which is a sole indicator of ring current intensity.

AGREEMENT WITH EXPLORER 45 OBSERVATIONS

The Volland-Stern type convection electric field model, described in the previous section, with the addition of the dependence of the electric field strength on the Kp index has been used to study various magnetospheric phenomena especially those measured by Explorer 45. Maynard and Chen (1975) were able to interpret with this model their observations from Explorer 45 of regions of isolated cold plasma. Grebowsky and Chen (1975) used this $\gamma = 2$ model to explain the general relation of the observed location of the nose events of Smith and Hoffman (1974) to the observed plasmapause location measured on the same satellite (Maynard and Cauffman, 1973) and predicted the spatial location of the nose by computing the forbidden region boundaries in the same manner as in Stern's (1975) analysis.

The shape of the nose structures in the energy-time spectrograms and its location just inside the plasmapause was studied by Cowley (1976) and Cowley and Ashour-Abdalla (1976) and they concluded that the observed noses cannot be modeled with any uniform dawn-dusk convection electric field since that field ($\gamma = 1$ in equation 5) predicts that the nose should penetrate down to much lower L-values than is observed. They suggested that the convection electric field may be shielded from the plasmasphere region so that the penetration could not occur. Ejiri et al. (1978) have noted that the intensity of the electric field inside the plasmapause is smaller with the Volland-Stern field and in fact the shielding effects can only be introduced if $\gamma > 1$. Cowley (1976) also pointed out that the particles may have been "lost" before they could penetrate very deeply, either by charge exchange or strong diffusion.

Thus Cowley's conclusions are not inconsistent with this $\gamma = 2$ model of Volland and Stern.

Intensity enhancements of the ring current electrons associated with VLF-emissions during geomagnetic storms and the energy dispersion of these enhancements have been explained by Maeda et al. (1978) using the computed electron trajectories given by this model (Ejiri, 1978). Additional progress was made by Ejiri et al. (1978) in the utilization of trajectories calculated in a static-electric field. They found that to explain the sequence of positions of nose structures during a magnetic storm, the location of particle fronts had to be calculated, taking into account the finite traveling time of newly-injected particles, instead of considering only the particle inner boundaries determined for $t = \infty$. Ejiri et al. (1978) noted that McIlwain's (1974) E3 or E3H electric field models correspond to a weak field and do not predict the plasmapause position inside the Explorer 45 orbit. Ejiri et al. (1979) also used the $\gamma = 2$ convection model for explaining the ion nose structure for both equatorially mirroring ions and those with other pitch angles. They examined the energy spectra and penetration distances for both electrons and ions in the post-midnight to morning hours local time.

ADDITION OF TIME-DEPENDENCE TO CONVECTION ELECTRIC FIELD

In the previous sections we have shown how the Volland-Stern convection electric field, Eq (3), can be related through Eqs (4) and (5) to the Kp index. The use of this index to parameterize convection boundaries is discussed by Kivelson (1976), principally for the uniform ($\gamma = 1$) dawn-dusk electric field, but also for the model we have been discussing and which Kivelson (1976) refers to as the VSMC (Volland-Stern-Maynard-Chen) model. While this model is more sophisticated than the $\gamma = 1$ model and it provides good agreement with a large data set (see previous section), one of the principal advantages is that it is a simple model and does not require large amounts of computer time to generate the particle trajectories described by Ejiri (1978). In keeping with this approach we have added a time dependence to this static electric field model in a very simple way. As shown by Maeda et al. (1978) the electric field intensity is related to Kp through a very smooth function (Figure 2). We merely use the time history of Kp, which is available to a wide user community, to determine the large scale convection electric field intensity. We interpolate the three-hourly values of Kp to get an hourly quasi-value called Kp' from which the electric field can be determined on an hourly basis. This is done under the gross assumption that the large scale convection electric field must change smoothly over the large areas considered or that at least the particles' response to the changing electric field can be, on average, represented by this type of field. In the previous work with this model (Ejiri et al. 1978, 1979) a static electric field was used with the particles moving in time along fixed trajectory paths (Figure 3).

With the addition of this time-varying electric field the trajectories themselves change in time as the particles move through the magnetosphere.

The utilization of a time-dependent electric field for particle convection is not a new idea (Kellogg, 1959). Roederer and Hones (1974) devised a time-dependent electric field model, composed of a time-dependent uniform dawn-dusk field component, a static component of the dawn-dusk and corotational fields, and a localized azimuthal field, to simulate the particle injections observed at the geo-synchronous orbit by ATS-5. McIlwain (1972) also pointed out that transient field changes are required to cause the observed particle injections to remain on stably trapped orbits.

In Figure 4 the Kp index is shown for the February 24-25, 1972, geomagnetic storm. The computed electric field intensity at 10 R_E, at midnight ($\phi = 0°$) determined from Kp' is shown in the upper portion. Note that after the initial Kp increase, the index decreased during the next 24 hours and then increased slightly from Kp = 2 to Kp = 3. During this period of Kp decrease the computed field weakens by an order of magnitude from a peak value of about 1 mV/m. In the next section we will use this time-varying convection $\vec{E}$ field in the computation of the motions of charged particles of various magnetic moments (both ions and electrons).

VISUAL DESCRIPTION OF PARTICLE MOTION

The addition of the time-varying convection $\vec{E}$ field to the trajectory traces of Ejiri (1978) shown in Figure 3, suggested to us that the most beneficial display technique is motion pictures which would provide the time dimension not only for the variation in electric field strength but also for the movement of the particles themselves. Computer-generated movies of storm "fronts" of injected particles of various magnetic moments have been produced and have been shown at scientific meetings (Smith et al., 1978). In the figures that follow some snap-shot frames of the movie titled "Convection of Magnetospheric Particles in a Time-Varying Electric Field" (Version 780919) are presented. The general characteristics and format of the movie frames (Figures 5-8) are:

1. Singly-charged particles are injected from a distance of 10 R_E and only equatorially mirroring particles are considered.
2. Injection is over a wide local time region around midnight and a uniform spacing of the injection points is assumed, except for the extra trajectories in small local time regions which are added in order to show which trajectories are "trapped". This will be discussed later.
3. The trajectories are not followed after they intersect the 10 R_E boundary.
4. The time history of the electric field intensity is shown in Figure 4. The field changes every hour and the particles will move during each hour under the field prescribed by Kp' shown on the individual movie frames.

5. The time, T, changes in the movie every 0.1 hour and a new injection of particles occurs every hour and is arbitrarily stopped after 20 injections.
6. The magnetic moment is conserved in each of the cases and is shown on the frames. The kinetic energy, E, of the particle at the time of injection at L = 10 is shown in the upper right-hand portion of the frame. The particles are energized in this injection process by cross-L drift.
7. The dotted shape is essentially the plasmapause, i.e. the last closed equipotential lines for this convection model. The size varies with Kp'. It should be noted that the shape of McIlwain's injection boundary (Mauk and McIlwain, 1974) normalized by the stagnation point at dusk coincides well with this shape, but that the unnormalized distance is well beyond this "plasmapause".
8. The dashed ellipse is the S^3-A (Explorer 45) orbit. The satellite is indicated by the "S" moving around the ~ 8 hour orbit.
9. In this version of the movie only the line segments of the trajectories since the last whole hour are shown. At T = 2.5 hours, for example, line segments of trajectories are shown for three injection fronts; each line shows where the particle has traveled since T = 2.0 hours.

In Figures 5-8 the trajectories for four selected magnetic moment cases are shown and are for the following μ's: 1) μ = 0.024, 2) μ = 0.065, 3) μ = 0.0 and 4) μ = -0.032, respectively where μ is given in units

of keV/γ. Cases 1 and 2 are for ions, case 3 for thermal particles and case 4 for electrons. In Figure 5 the injection energy at L = 10 is 0.75 keV and when the ions have reached L = 5 they have been energized to 6 keV. The six snapshots in Figure 5a are taken at two hour intervals starting at T = 2.5 hours. The snapshots in Figure 5b are shown at four hour intervals. It can be seen that the particles injected at local times within an hour or two of midnight are much slower in moving around the earth than those injected at local times away from midnight. At T = 2.5 hours certain trajectories have intersected L = 10 on the day side before other trajectories have crossed L = 6 near midnight. A fine line separates those trajectories going around the earth on the dawn side from those going around (counter to corotation) through the dusk hours. The trajectories begin to intersect the S^3-A orbit after T = 4.5 hours and by T = 8.5 hours have moved to the lower altitude regions traversed by the satellite. Note that, at T = 8.5 hours and corresponding to the high Kp' value of 5.3, the particles at midnight convect from L = 10 to L = 6.5 within 30 minutes. The plasmapause has contracted to L = 2.5 at dawn and L = 4 at dusk. By 12.5 hours the particles are convected into L = 3 on the dusk side and are well inside the plasmapause. Twenty separate injections are simulated and then arbitrarily stopped. It can be seen in the frames at T = 20.5 and T = 24.5 hours that certain of the trajectories are beginning to appear to be trapped. Even with the large number of simulated trajectories only a very few are actually trapped, and even at T = 24.5 hours those particles have not yet made a full revolution around the earth. As shown in Figure 4 the Kp index continued to decrease to a value of 2, which is shown at T = 32.5 hours in Figure 5b. At this time the "plasmapause" had expanded to 7 R_E at dusk and

most of the remaining trajectories were within this plasmasphere. An interesting effect is that even at this relatively low Kp value there exists a stream of particles near noon which are being convected toward the front side L = 10 boundary. It is as if these particles are being kicked out of their trapped orbits by the changing $\vec{E}$ field. The electric field is subsequently enhanced and this effect persists for the remaining time up to the full 48 hours considered in the movie, but not shown in Figure 5. The other interesting and obvious point is the particle diffusion effects produced by this model and most easily seen at the later times.

In Figure 6 the injection energy of the ions is 2.00 keV, and these particles reach 31.25 keV at L = 4. The principal difference is that these particles move much faster. At T = 16.5 hours certain of the trajectories are clearly trapped and the time to make one revolution of the earth was only about 15 hours. These ions, on the other hand, do not penetrate as deep as the lower energy ions. By T = 24.5 hours there is the clearly established ring of particles but also the "noon" convection flow which was described for Figure 5.

The trajectories for the thermal particles (μ = 0.0) are shown in Figure 7 at a six-hour spacing starting at T = 4.5 hours. These particles convect in further from midnight before they begin their corotational drifts. The trajectories begin to intersect the S^3-A orbit near L = 5 in the T = 10.5 frame and it takes well over a day for the injected particles to reach the outbound portion of the orbit at 1600 MLT after they have gone around the earth on the dawn side. The trajectories are

well bounded inside the "plasmasphere" after about 30 hours except for the few trajectories which exit and go out the front of the boundary near 1400 MLT.

The one example of electron trajectories is shown in Figure 8 for electrons injected at L = 10 with kinetic energy of 1.0 keV. Figure 8a shows six snapshots at two hour intervals and 8b shows the six at four hour intervals. While a few of the trajectories originate and exit on the dusk side, the vast majority travel through the dawn hours even though they might have originated on the dusk side of midnight. There is a heavy concentration of trajectories in the morning hours starting at about 6 R_E at T = 4.5 hours and moving closer to the earth as the electric field increases. As seen in Figure 8a only a couple of trajectories intersect the S^3-A orbit (at L = 5 inbound) during those hours and the trajectories do not begin to intersect the outbound portion of the orbit until about 16.5 hours, after they have nearly encircled the earth. Within about a day there is formed a ring of trapped electrons whose trajectories are at or beyond the "plasmapause" location. It is not until the electric field has decreased (at T = 32.5 hours) to a low level that the electrons are substantially inside the plasmapause and only on the dusk side. The electrons do become trapped and exhibit the "dumping" of particles from the "trapped" orbits into the noon convection stream as described also for the ions.

As shown in the figures above there exist narrow local time regions at L = 10 from which the subsequently trapped particles are injected onto stable orbits. The trapping depends on the electric field time history and hence the local time region of injection varies according to

the magnetic storm conditions. Also the region varies in local time according to the magnetic moment of the injected particles. This dependence is shown in Figure 9 for two geomagnetic storms, the February 1972 storm which we have previously discussed and the July 29, 1977 storm shown for comparison. The region from which the trapped particles emerge varies from pre-midnight (~ 21 MLT) for large negative μ's (electrons) to post midnight (~ 02 MLT) for large positive μ's (ions). The exact dependence is of course coupled directly to the convection model we are using, but this could be a good additional test for this general convection formulism.

DISCUSSION

The basic convection model described in this paper agrees well with the Explorer 45 results. The comparison of the time-dependent electric field extension of this model to the data has not yet been made, however. The model does provide for the trapping of the particle trajectories which was not possible in the static convection electric field case. It is an analytically simple model to use and can provide the foundation for more refined large-scale convection models especially one which takes into account the tilt and the tail-like geometry of the geomagnetic field. It should also be emphasized that the large scale convection electric field which has been used in this model is a smooth power-law electric field and it does not provide for the rapid plasma flows observed at subauroral latitudes in the topside ionosphere (Shiro et al., 1978), nor does it explicitly include the type of large (20-30 mV/m) transient electric fields which occur during short periods (30-60 sec.) and which have been observed, for example, on GEOS (Pedersen and Grard, 1979). The overall magnetude of the convection electric field, however, does agree with the average field (~ 1.0 mV/m) measured on GEOS (Pedersen and Grard, 1979) and with the field derived from the particle velocity distributions obtained from ISEE (Frank et al., 1978). It is, of course, not the only electric field model currently in use (Stern, 1977) and other models such as McIlwain's (1974) based on ATS-5 results and the self-consistent modeling described by Wolf (1975) must also be considered. The Wolf model (Harel et al., 1979), for example, is more detailed and takes into account the boundary currents and ionospheric coupling effects.

It is expected that the computer-generated movie display technique, which we have employed, will be increasingly used in the development of the various quantitative magnetospheric models. This technique provides an exceptional educational tool for magnetospheric physics, and future studies of particle dynamics in the magnetosphere will require this technique as an analytical tool due to the increased complexity of the analysis with the recent addition of time-dependent electric fields.

REFERENCES

Axford, W. I., Magnetospheric convection, Rev. Geophys. Space Phys. 7, 421-459, 1969.

Axford, W. I., and C. O. Hines, A unifying theory of high-latitude geophysical phenomena and geomagnetic storms, Can. J. Phys., 39, 1433-1464, 1961.

Brice, N. M., Bulk motion in the magnetosphere, J. Geophys. Res., 72, 5193-5211, 1967.

Carpenter, D. C. and C. Park, On what ionospheric workers should know about the plasmapause-plasmasphere, Rev. Geophys. Space Phys., 11, 133-154, 1973.

Chappell, C. R., The convergence of fact and theory on magnetospheric convection, in Correlated Interplanetary and Magnetospheric Observations, edited by D. E. Page, pp 277-295, D. Reidel, Dordrecht, Netherlands, 1974.

Chen, A. J., Penetration of low-energy protons deep into the magnetosphere, J. Geophys. Res., 75, 2458-2467, 1970.

Cowley, S. W. H., Energy transport and diffusion, in Physics of Solar Planetary Environments, edited by D. J. Williams, pp 582-607, Proceedings of the International Symposium on Solar-Terrestrial Physics, American Geophysical Union, Washington, D.C., 1976.

Cowley, S. W. H. and M. Ashour-Abdalla, Adiabatic plasma convection in a dipole field: Proton forbidden-zone effects for a simple electric field model, Planet. Space Sci., 24 821-833, 1976.

Dungey, J. W., Interplanetary magnetic field and the auroral zones, Phys. Rev. Letters, 6, 47-48, 1961.

Ejiri, M., Trajectory traces of charged particles in the magnetosphere, J. Geophys. Res., 83, 4798-4810, 1978.

Ejiri, M., R. A. Hoffman and P. H. Smith, The convection electric field model for the magnetosphere based on Explorer 45 observations, J. Geophys. Res., 83, 4811-4815, 1978.

Ejiri, M., R. A. Hoffman and P. H. Smith, Energetic particle penetrations into the inner magnetosphere, to be published in, J. Geophys. Res., (Preprint NASA/GSFC X-625-77-254), 1979.

Frank, L. A., K. L. Ackerson, R. J. De Coster, and B. G. Burek, Three-dimensional plasma measurements within the earth's magnetosphere, to be published in, Space Sci. Rev., presented at 13th ESLAB Symposium, Innsbruck, Austria, 1978.

Grebowsky, J. M. and A. J. Chen, Effects of convection electric field on the distribution of ring current type protons, Planet. Space Sci., 23, 1045-1052, 1975.

Harel, M., R. A. Wolf, P. H. Reiff, and M. Smiddy, Computer modeling of events in the inner magnetosphere, Quantitative Modeling of the Magnetospheric Processes, Geophys. Monogr. Ser., vol. 21, edited by W. P. Olson, AGU, Washington, D.C. 1979.

Heppner, J. P., Electric field variations during substorms: OGO-6 measurements, Planet. Space Sci., 20, 1475-1498, 1972.

Jaggi, R. K., and R. A. Wolf, Self-consistent calculation of the motion of a sheet of ions in the magnetosphere, J. Geophys. Res., 78, 2852-2866, 1973.

Johnson, R. G., R. D. Sharp, and E. G. Shelley, Observations of ions of ionospheric origin in the storm-time ring current, Geophys. Res. Letters, 4, 403-406, 1977.

Kavanagh, L. D. Jr., J. W. Freeman, Jr., and A. J. Chen, Plasma flow in the magnetosphere, J. Geophys. Res., 73, 5511-5519, 1968.

Kellogg, P. J., Van Allen radiation of solar origin, Nature, 183, 1295-1297, 1959.

Kivelson, M. G., Magnetospheric electric fields and their variation with geomagnetic activity, Rev. Geophys. Space Phys., 14, 189-197, 1976.

Maeda, K., N. K. Bewtra, and P. H. Smith, Ring current electrons trajectories associated with VLF-emissions, J. Geophys. Res., 83, 4339-4346, 1978.

Mauk, B. H. and C. E. McIlwain, Correlation of Kp with the substorm-injected plasma boundary, J. Geophys. Res., 79, 3193-3196, 1974.

Maynard, N. C., and D. P. Cauffman, Double-floating probe measurements on S^3-A, J. Geophys. Res., 78, 4745-4750, 1973.

Maynard, N. C., and A. J. Chen, Isolated cold plasma regions: Observations and their relation to possible production mechanisms, J. Geophys. Res., 80, 1009-1013, 1975.

McIwain, C. E., Plasma convection in the vicinity of the geosynchronous orbit, in Earth's Magnetospheric Processes, edited by B. M. McCormac, p 268-279, D. Reidel, Dordrecht, Netherlands, 1972.

McIwain, C. E., Substorm injection boundaries, in Magnetospheric Physics, edited by B. M. McCormac, pp 143-154, D. Reidel, Dordecht, Netherlands, 1974.

McIwain, C. E., Auroral electron beams near the magnetic equator, Nobel Symposium Proceedings, Plenum Publishing Co., London, 1975.

Mead, G. D., Deformation of the geomagnetic field by the solar wind, J. Geophys. Res., 69, 1181-1195, 1964.

Nishida, A., and T. Obayashi, Magnetosphere convection, in Critical Problems of Magnetospheric Physics, edited by E. R. Dyer, p. 179, Inter-Union Commission on Solar-Terrestrial Physics Secretariat, National Academy of Sciences, Washington, D. C., 1972.

Pedersen, A., and R. Grard, A review of dc electric field measurements performed on GEOS, Quantitative Modeling of the Magnetospheric Processes, Geophys. Monogr. Ser., vol. 21, edited by W. P. Olson, AGU, Washington, D.C., 1979.

Roederer, J. G., Dynamics of Geomagnetically Trapped Radiation, Springer, New York, 1970.

Roederer, J. G. and E. W. Hones, Jr., Motion of magnetospheric particle clouds in a time-dependent electric field model, J. Geophys. Res., 79, 1432-1438, 1974.

Shelley, E. G., R. G. Johnson, and R. D. Sharp, Satellite observations of energetic heavy ions during a geomagnetic storm, J. Geophys. Res., 77, 6104-6110, 1972.

Shiro, R. W., R. A. Heelis, and W. B. Hanson, Ion convection and the formation of the mid-latitude F region ionization trough, J. Geophys. Res., 83, 4255-4264, 1978.

Smith, P. H., and R. A. Hoffman, Direct observation in the dusk hours of the characteristics of the storm time ring current particles during the beginning of magnetic storms, J. Geophys. Res., 79, 966-971, 1974.

Smith, P. H., R. A. Hoffman, and N. K. Bewtra, A visual description of the dynamical nature of magnetospheric particle convection in a time-varying electric field, EOS, 59, p. 361, 1978.

Stern, D. P., Models of the earth's electric field, NASA/GSFC X-602-74-159, May 1974.

Stern, D. P., The motion of a proton in the equatorial magnetosphere, J. Geophys. Res., 80, 595-599, 1975.

Stern, D. P., Large-scale electric fields in the earth's magnetosphere, Rev. Geophys. Space Phys., 15, 156-194, 1977.

Vasyliunas, V. M., The interrelationship of magnetospheric processes, in Earth's Magnetospheric Processes, edited by B. M. McCormac, pp 29-38, D. Reidel, Dordrecht, Netherlands, 1972.

Volland, H., A semiempirical model of large-scale magnetospheric electric fields, J. Geophys. Res., 78, 171-180, 1973.

Wolf, R. A., Effect of ionospheric conductivity on convective flow of plasma in the magnetosphere, J. Geophys. Res., 75, 4677-4698, 1970.

Wolf, R. A., Ionosphere-magnetosphere coupling, Space Sci. Rev., 17, 537-562, 1975.

FIGURE CAPTIONS

Figure 1. Normalized large scale convection electric field of the Volland-Stern type with $\gamma = 2$. The vectors are shown in the equatorial plane in L, MLT coordinates.

Figure 2. Parameters of the convection electric field plotted against Kp: (1) A(Kp) given by equation 5, (2) E, the electric field at L = 10 and at midnight ($\phi = 0$), and (3) L_0, the radial distance of the duskside stagnation point from the earth's center in the equatorial plane in earth radii (from Fig. 2 Maeda et al. (1978)).

Figure 3. Particle flow patterns for $\mu = 0.02$ keV/γ particles with 90° pitch angles under a static electric field from Fig. 9 of Ejiri (1978) for Kp = 4. The "*" are the hour markers along the fixed trajectories. This shows the particle locations after 20 hours of motion from injection.

Figure 4. Kp index for 48 hours during the February 24, 1972, geomagnetic storm. The computed electric field intensity at 10 R_E, at midnight ($\phi = 0°$) determined from one hour interpolated values of Kp is given in the upper portion and the time agrees with the value of T given in Figures 5-8.

Figure 5. Selected snapshot frames from the movie "Convection of Magnetospheric Particles in a Time-Varying Electric Field" (Version 780919) for particles of magnetic moment, $\mu = 0.024$ keV/γ. The configuration at twelve times, T, are shown in (a) and (b). (See text for detailed discussion.)

Figure 6. Same as Figure 5, but for μ = 0.065 keV/γ particles. Six time periods are shown.

Figure 7. Same as Figure 5, but for μ = 0.0 keV/γ particles with six time periods shown.

Figure 8. Same as Figure 5, but for μ = -0.032 keV/γ particles (electrons). The configuration at twelve times, T, are shown in (a) and (b).

Figure 9. Magnetic local time of injection at L = 10 for those trajectories which subsequently get "trapped" around the earth using the described convection model. The MLT varies with the magnetic moment of the particles and with the time history of the convection electric field (Kp). Two magnetic storms, February 24, 1972 and July 29, 1977, are shown.

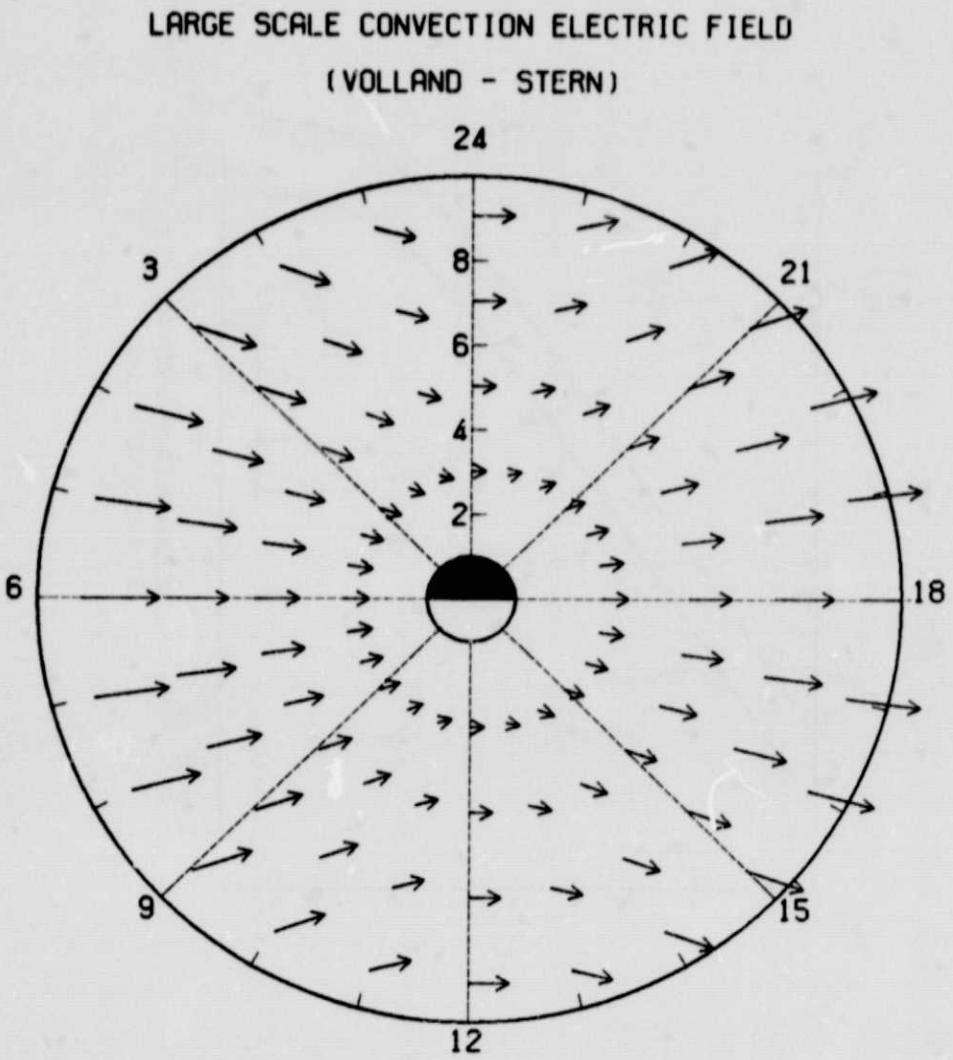

FIGURE 1

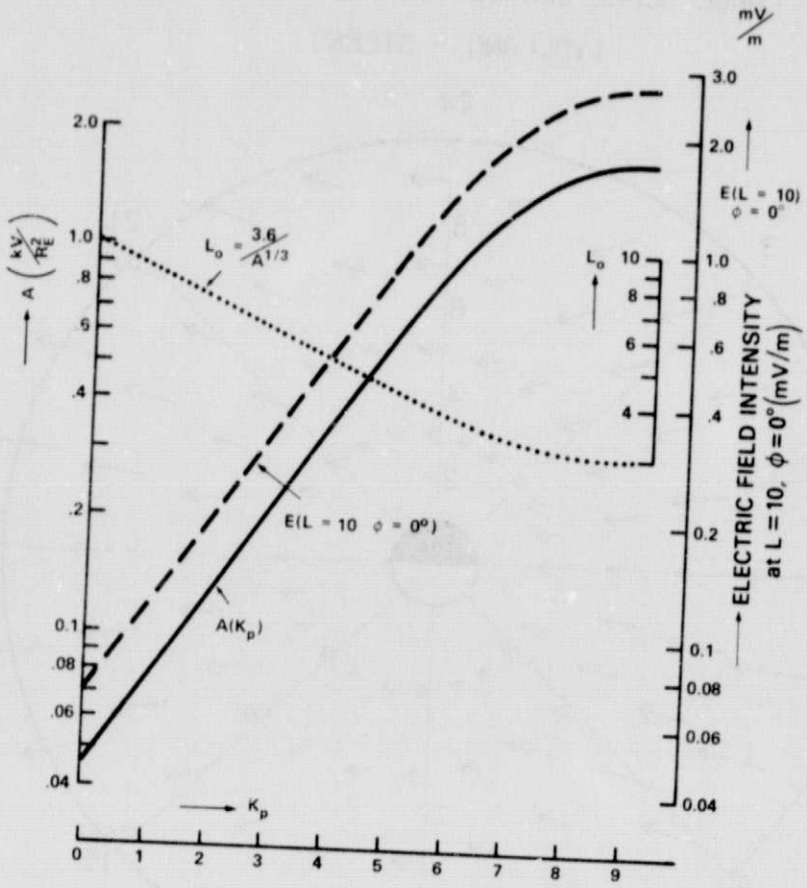
mV/m
3.0
2.0
E(L = 10)
φ = 0°
2.0
1.0
.8
.6
.4
.2
0.1
.08
.06
.04
A (kV/R_E²)
L_o = 3.6/A^1/3
L_o
10
8
6
4
1.0
.8
.6
.4
0.2
0.1
0.08
0.06
0.04
ELECTRIC FIELD INTENSITY
at L = 10, φ = 0° (mV/m)
E(L = 10 φ = 0°)
A(K_p)
K_p
0
1
2
3
4
5
6
7
8
9

FIGURE 2

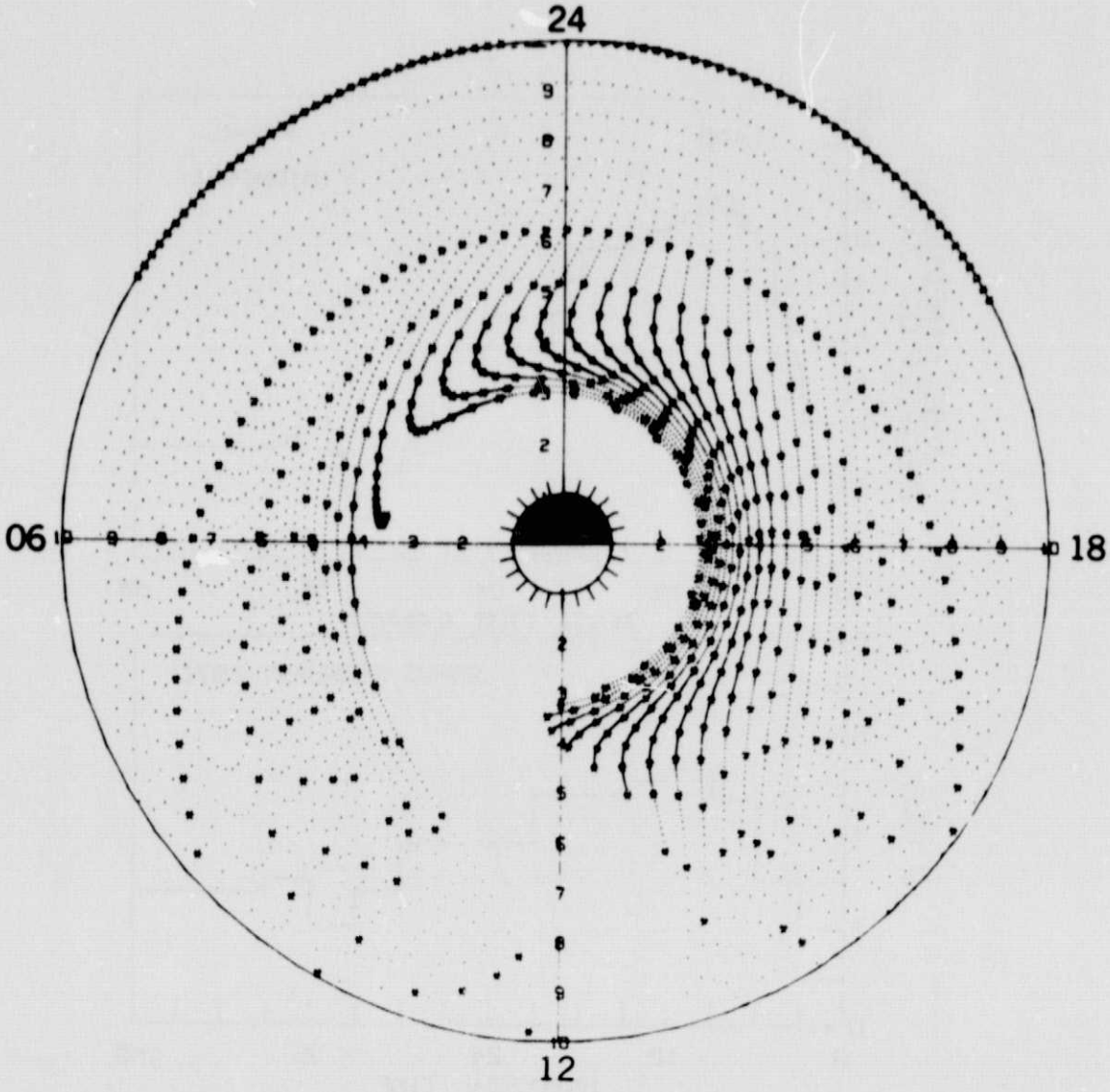

FIGURE 3

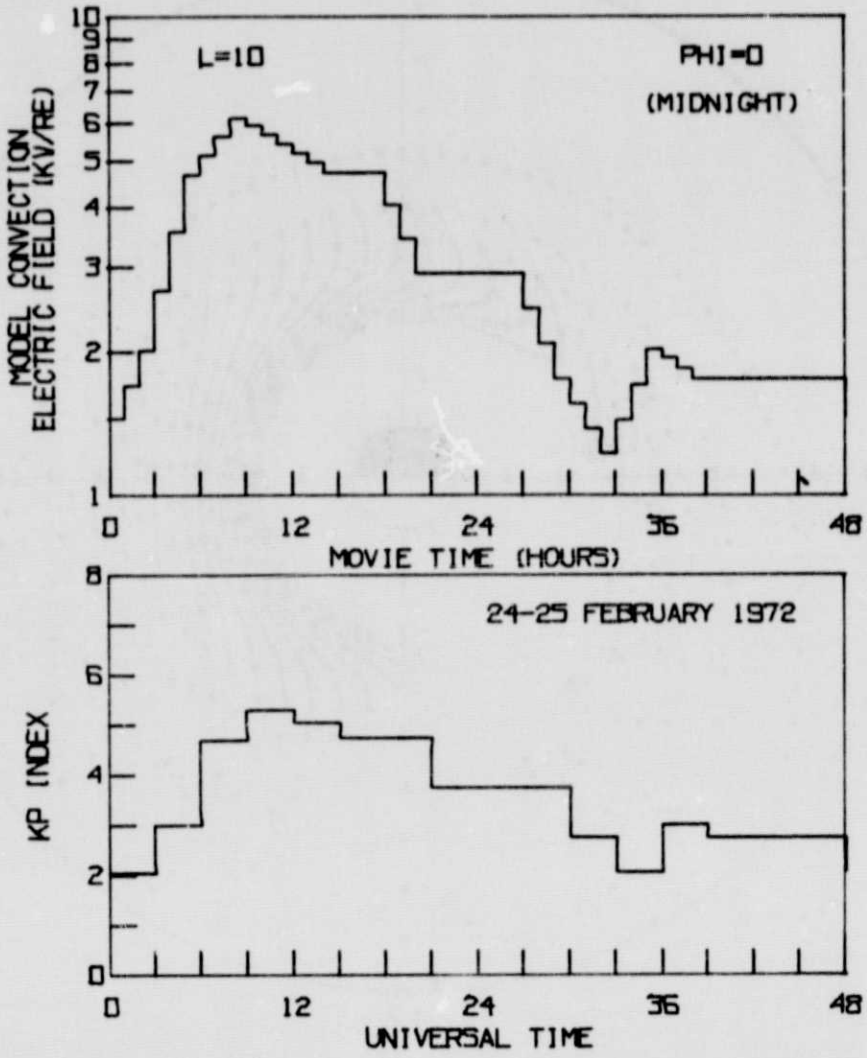
L=10
PHI=0
(MIDNIGHT)
MODEL CONVECTION ELECTRIC FIELD (KV/RE)
10
9
8
7
6
5
4
3
2
1
0
12
24
36
48
MOVIE TIME (HOURS)
24-25 FEBRUARY 1972
KP INDEX
8
6
4
2
0
0
12
24
36
48
UNIVERSAL TIME

FIGURE 4

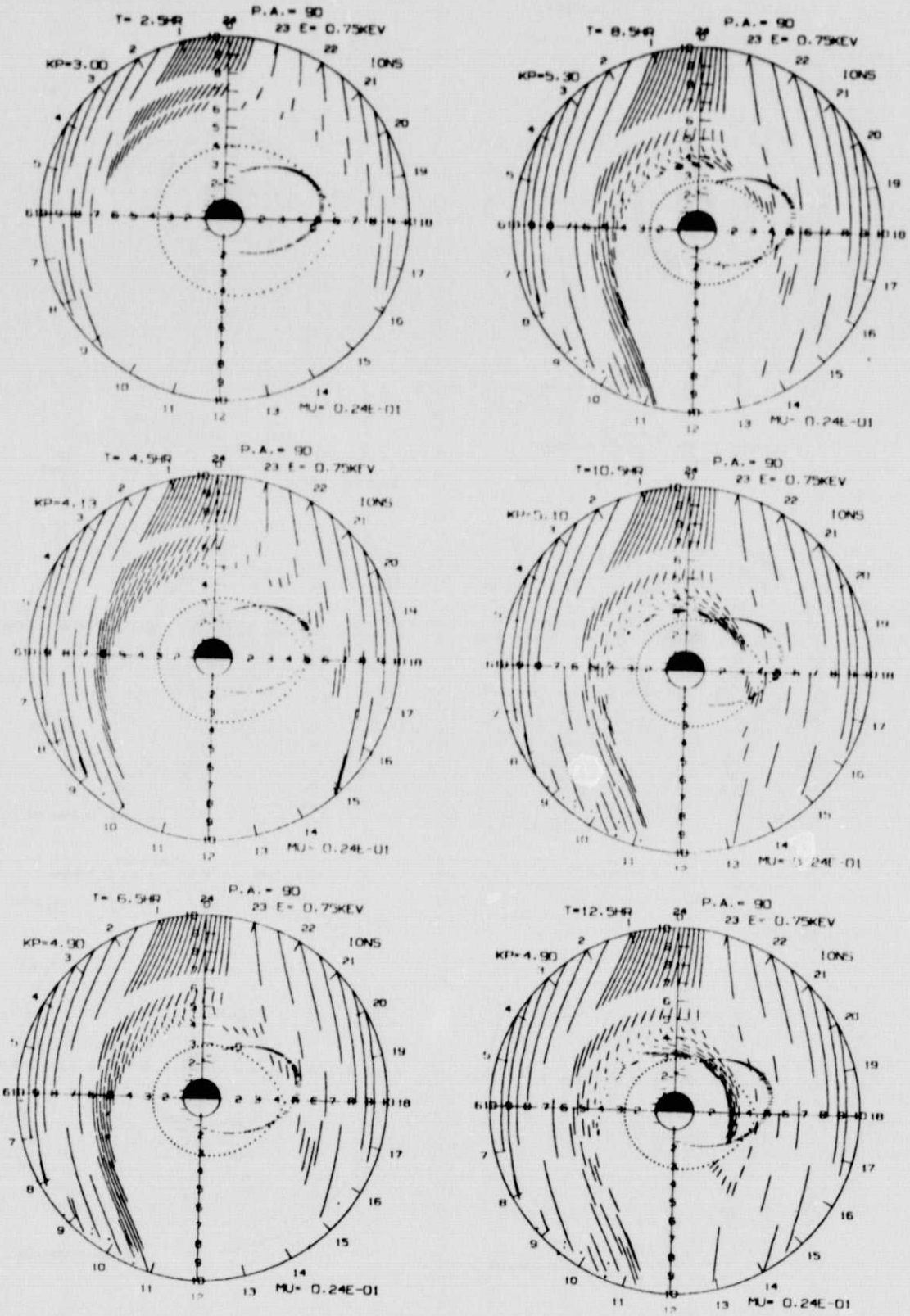

FIGURE 5a

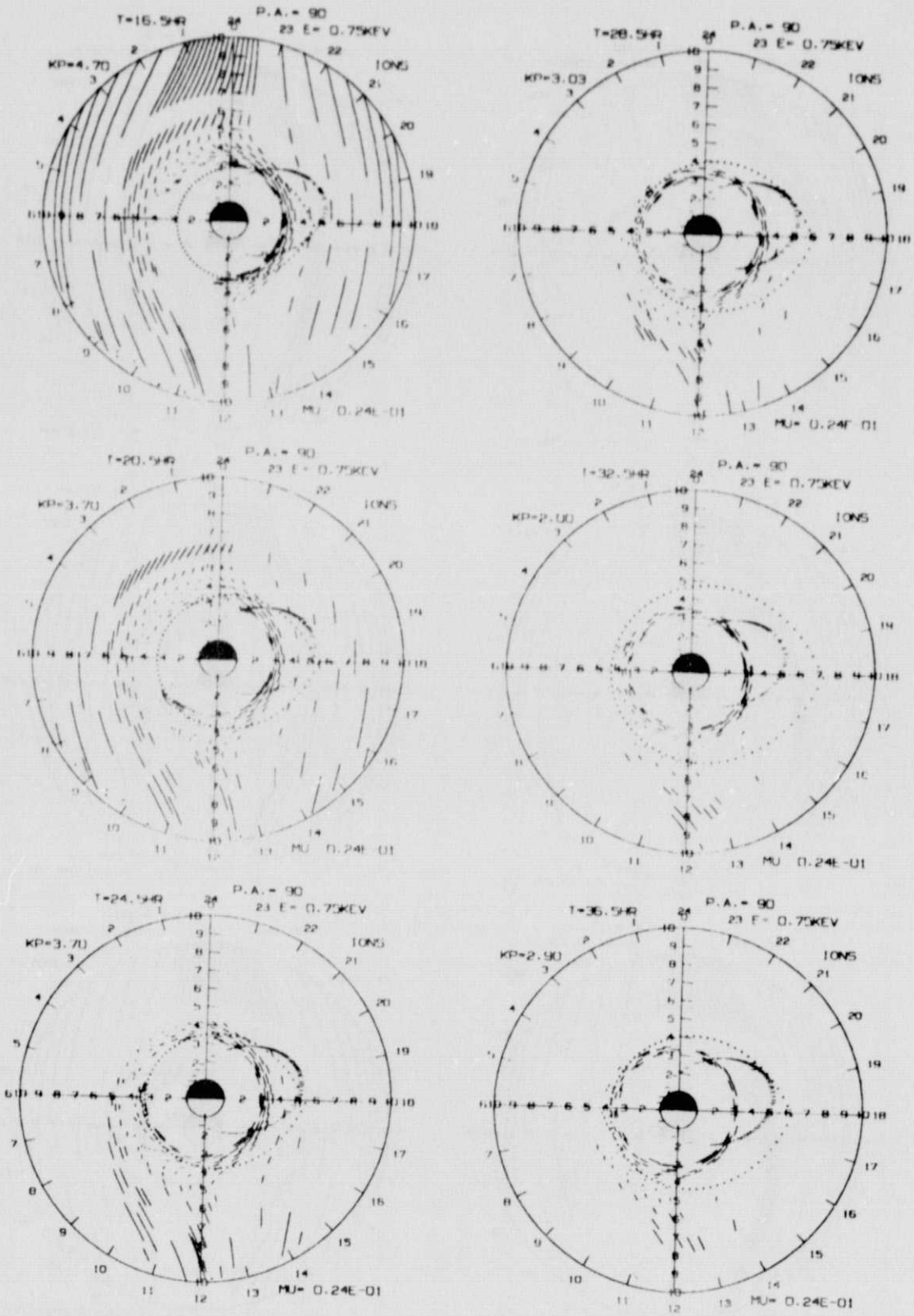
T=16.5HR
P.A.= 90
23 E= 0.75KEV
KP=4.70
IONS
MU= 0.24E-01
T=28.5HR
P.A.= 90
23 E= 0.75KEV
KP=3.03
IONS
MU= 0.24E-01
T=20.5HR
P.A.= 90
23 E= 0.75KEV
KP=3.71
IONS
MU= 0.24E-01
T=32.5HR
P.A.= 90
23 E= 0.75KEV
KP=2.00
IONS
MU= 0.24E-01
T=24.5HR
P.A.= 90
23 E= 0.75KEV
KP=3.71
IONS
MU= 0.24E-01
T=36.5HR
P.A.= 90
23 E= 0.75KEV
KP=2.90
IONS
MU= 0.24E-01

FIGURE 5b

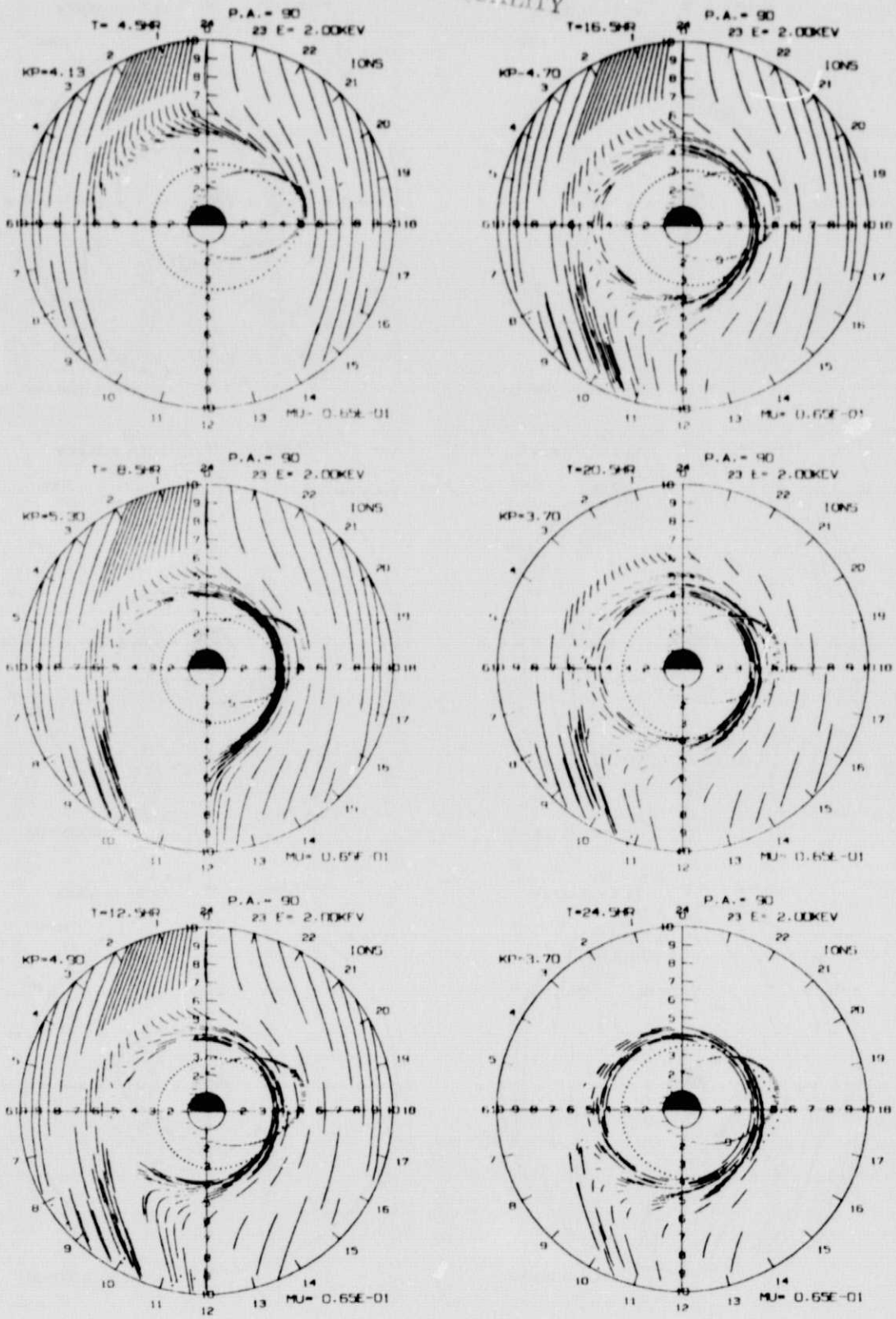

FIGURE 6

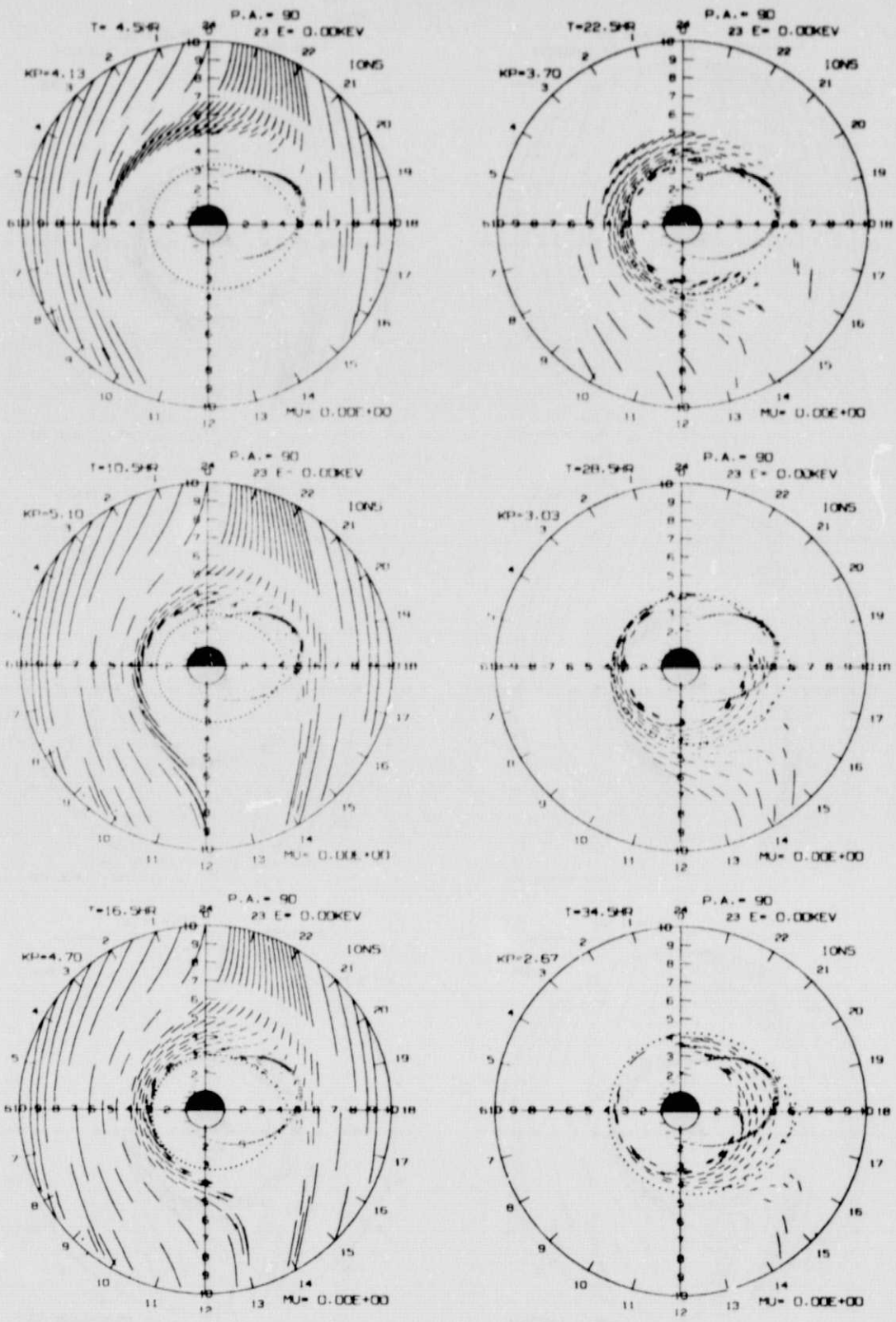
T= 4.54R
P.A.= 90
23 E= 0.00KEV
IONS
KP=4.13
MU= 0.00E+00
T=22.54R
P.A.= 90
23 E= 0.00KEV
IONS
KP=3.70
MU= 0.00E+00
T=10.54R
P.A.= 90
23 E= 0.00KEV
IONS
KP=5.10
MU= 0.00E+00
T=28.54R
P.A.= 90
23 E= 0.00KEV
IONS
KP=3.03
MU= 0.00E+00
T=16.54R
P.A.= 90
23 E= 0.00KEV
IONS
KP=4.70
MU= 0.00E+00
T=34.54R
P.A.= 90
23 E= 0.00KEV
IONS
KP=2.67
MU= 0.00E+00

FIGURE 7

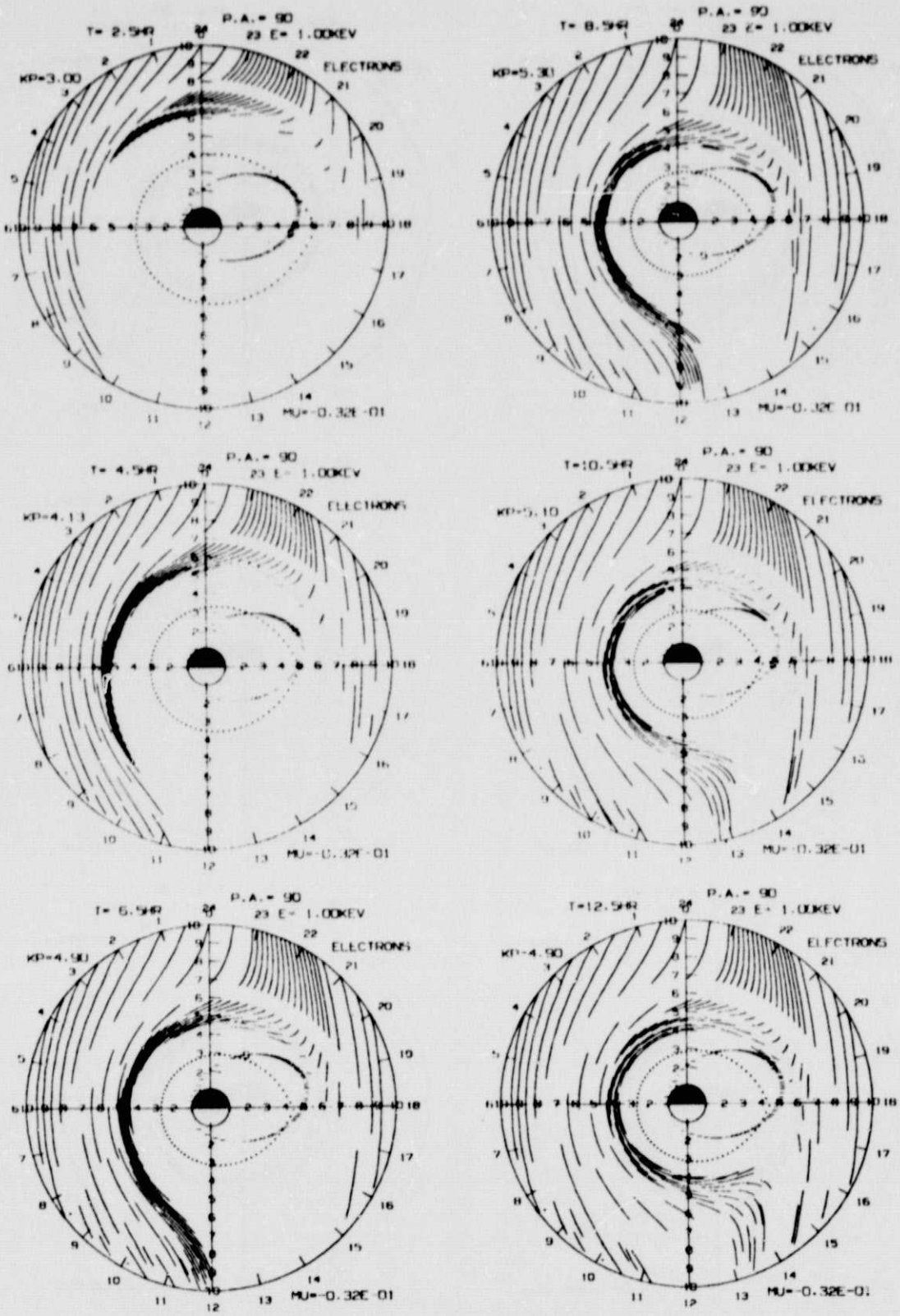

FIGURE 8a

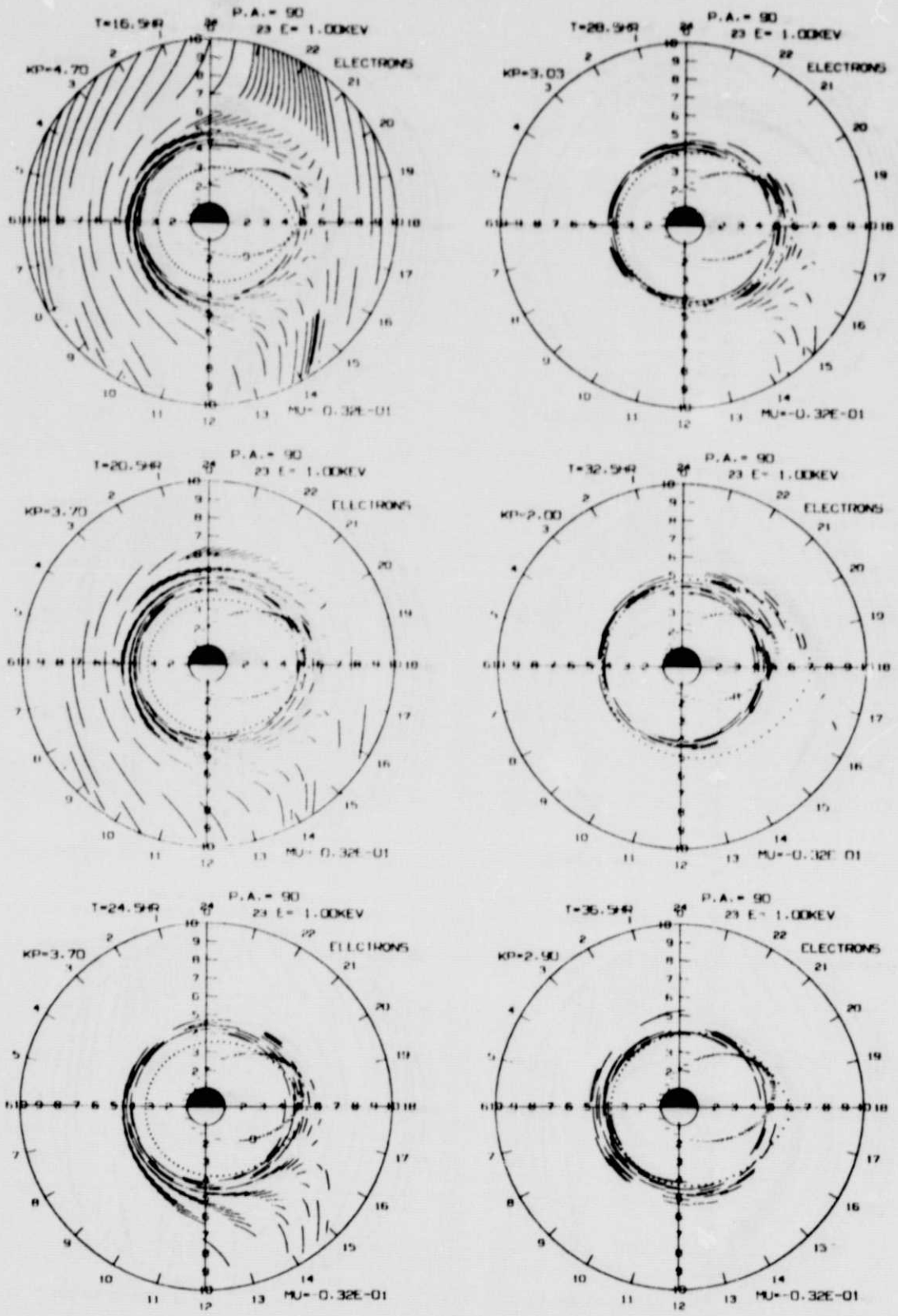
T=16.5HR
P.A.= 90
23 E= 1.00KEV
KP=4.70
ELECTRONS
MU= 0.32E-01
T=28.5HR
P.A.= 90
23 E= 1.00KEV
KP=3.03
ELECTRONS
MU=-0.32E-01
T=20.5HR
P.A.= 90
23 E= 1.00KEV
KP=3.70
ELECTRONS
MU= 0.32E-01
T=32.5HR
P.A.= 90
23 E= 1.00KEV
KP=2.00
ELECTRONS
MU=-0.32E-01
T=24.5HR
P.A.= 90
23 E= 1.00KEV
KP=3.70
ELECTRONS
MU=-0.32E-01
T=36.5HR
P.A.= 90
23 E= 1.00KEV
KP=2.50
ELECTRONS
MU=-0.32E-01

FIGURE 8b

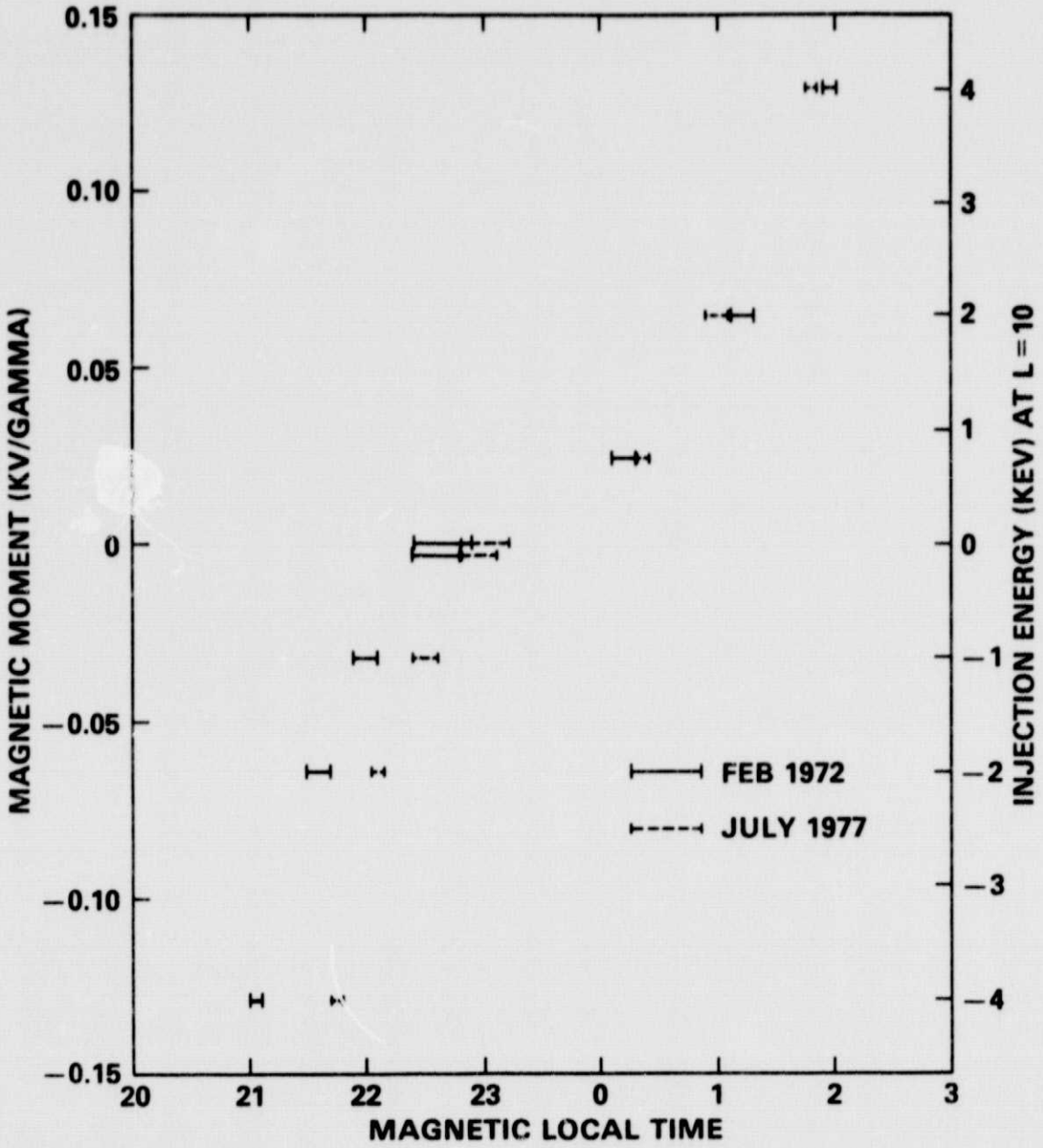

FIGURE 9